

Solid-State Organization and Morphological Partitioning in Polyoxymethylene-Based Copolymers: A Solid-State NMR and WAXS Study

Cédric Lorthioir,^{*,†} Françoise Lauprêtre,[†] Karthikeyan Sharavanan,^{‡,§}
Ronald F. M. Lange,[§] Philippe Desbois,[§] Michel Moreau,[‡] and Jean-Pierre Vairon[‡]

Laboratoire de Recherche sur les Polymères (CNRS-UMR 7581), 2-8 rue Henri Dunant, 94320 Thiais, France; Laboratoire de Chimie des Polymères (CNRS-UMR 7610), Université Pierre et Marie Curie, Case 185 T44 E1, 4 Place Jussieu, 75252 Paris Cedex 05, France; and BASF Research, GKT/U B1, D-67056 Ludwigshafen, Germany

Received October 30, 2006; Revised Manuscript Received May 3, 2007

ABSTRACT: The solid-state organization of copolymers based on methylene oxide (MO) units and tetramethylene oxide (T) units, with T unit contents ranging between 0.9 and 10.0 mol %, is investigated by the combined use of solid-state NMR, WAXS, and DSC experiments. In these semicrystalline copolymers, the T units can be viewed as linear defects inserted along linear poly(oxymethylene) chains. As expected, the insertion of T units induces a significant decrease of both crystallinity and crystallite size: a large part of T units is located in the amorphous domains. However, some T units can also be detected within the crystalline domains and/or the interfacial regions with the amorphous phase. More precisely, the amount of T units at both sides of the noncrystalline/crystalline interfaces seems to be much higher than the T units in the interior of the crystallites. At the lowest T unit content (0.9 mol %), the composition averaged over both interfacial and crystalline phases appears to be identical to the composition of the amorphous phase. When the comonomer content increases, the amount of T units in the interfacial and crystalline zones becomes higher and higher while the partitioning coefficient of the T units in these domains tends to a limiting value of 0.40.

1. Introduction

Poly(oxymethylene) (POM), also known commonly as polyacetal, has been used as an engineering plastic since 1960. Possessing high tensile, impact, and compression strength along with good abrasion and wear resistance, it became a typical alternative to metals for various applications in the automobile and electronics industry as gear boxes and computer components.^{1–3} Further household applications like door handles and toys brought this plastic right into people's homes.

Because of its regular chemical structure, POM usually displays high degrees of crystallinity of about 65%, which is the highest crystallinity observed in performance polymers. The high crystallinity gives the polymer its excellent wear resistance together with its high rigidity, tensile strength, and good dimensional stability.

On the other hand, POM homopolymers are thermally unstable and tend to depolymerize, starting at the unstable hemiformal hydroxyl group liberating formaldehyde by an "unzipping" mechanism.⁴ One possible strategy to prevent this unzipping process consists in transforming the polymer chains by a suitable end-capping method.⁴ An alternate way to obtain thermally stable POM-based materials is to synthesize a copolymer by using trioxane with cyclic acetal comonomers like ethylene oxide, 1,3-dioxolane, or 1,3-dioxepane.⁴

For these copolymers mainly composed of methylene oxide units, the localization of the comonomer units within the semicrystalline organization displayed by the copolymers is a central feature since it should significantly influence the

mechanical properties of these materials. In particular, one of the first questions to be addressed concerns the possibility for these comonomer units to be inserted within the crystalline domains. If this is the case, the relevant effect to be considered then is the partitioning of these units between both amorphous and crystalline regions. This effect is usually quantified by means of the crystalline partitioning coefficient, P_{CR} , defined as the ratio between the concentration of comonomer units within the crystalline phase and the overall concentration of these units in the whole semicrystalline copolymer.⁵ A P_{CR} value close to 0 indicates that the comonomer units considered tend to be excluded from the crystalline lattice and should induce a significant reduction of both degree of crystallinity and crystallite sizes, thus affecting the mechanical performances of the corresponding material. In addition, the effective fraction of comonomer units located within the amorphous phase, also directly related to the parameter P_{CR} , should influence the segmental mobility of amorphous polymer (sub)chains and, as a consequence, the mechanical properties displayed by these copolymers. Of course, the situation is much more complex, and additional parameters have to be taken into account to get a deep understanding of the structure/mechanical properties relationships. In particular, for the amorphous phase, the copolymer microstructure, the interaction parameter between both kinds of repeat units, and the glass transition temperature of the homopolymers corresponding to each type of repeat units should be considered. As far as the crystalline part is concerned, in addition to the crystallinity and the typical size of the crystalline regions, the nature of the crystalline morphology should also be considered. Indeed, for a copolymer constituted of A and B monomer units, a crystalline lattice of the same nature as the one formed by a neat homopolymer of A (B) will be obtained for a low content of B units (A units). However, in

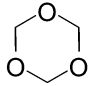
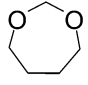
* Corresponding author: Tel +33 1 49 78 13 08, Fax +33 1 49 78 12 08, e-mail lorthioir@glvt-cnrs.fr.

[†] CNRS-UMR 7581.

[‡] CNRS-UMR 7610.

[§] BASF Research.

Table 1. Comonomers Used and Corresponding Repeat Units in the Copolymers

Comonomers			Copolymers: Repeat units		
1,3,5-trioxane	TOX		methylene oxide	MO	$-\text{CH}_2-\text{O}-$
1,3-dioxepane	DXP		tetramethylene oxide	T	$-(\text{CH}_2)_4\text{O}-$

the intermediate composition range, an intermediate crystalline organization may be observed. Such a behavior has been suggested in the case of ethylene and vinyl alcohol copolymers: for vinyl alcohol contents ranging from 20 to 60 mol %, a pseudohexagonal crystalline lattice was proposed, differing from the orthorhombic lattice usually observed for neat poly(ethylene) and from the monoclinic lattice of neat poly(vinyl alcohol).⁶ Last, in addition to both crystalline and amorphous phases mentioned previously, the description of the solid-state organization of semicrystalline copolymers should also take into account the interfacial regions. These regions include the so-called “constrained” amorphous phase, related to amorphous chain segments that are constrained by the presence of crystallites. These constrained chain units exhibit a slower segmental mobility than the purely amorphous subchains. In this respect, the constrained amorphous phase plays a significant role in the mechanical behavior of semicrystalline systems. Therefore, the localization of the comonomer units within the semicrystalline structure is a relevant point to be addressed in order to get a better understanding of the correlations between the chemical structure, the solid-state organization, and the mechanical properties of these copolymers.

The localization of comonomer units within semicrystalline copolymers or chain defects and chain ends within semicrystalline homopolymers has attracted a lot of interest, and the corresponding studies were mainly based on DSC or wide-angle X-ray scattering (WAXS) investigations. Though very useful, these techniques do not allow a direct and unambiguous localization of the comonomers, chain defects, or chain ends in the crystalline, constrained amorphous, and amorphous phases. In contrast, based on an approach proposed by VanderHart et al., solid-state NMR has proved to be successful in recording the ¹³C NMR spectra of both crystalline and noncrystalline regions of semicrystalline polymers.⁷ These experiments also permit to determine the crystalline partitioning coefficient related to the comonomers, chain defects, or chain ends of interest, provided they give a well-resolved resonance line on the ¹³C NMR spectra. Such solid-state NMR investigations have been carried out on various random copolymers,^{5,8–10} and very different behaviors, depending on the systems considered, have been reported. As expected, the size of the defects plays a key role in their potential insertion in the crystal lattice. In random copolymers of ethylene and α -olefins, for instance, it has been shown that small-size defects such as methyl or ethyl branches can be incorporated within the crystallites,¹⁰ while larger branches are fully excluded. Similarly, in random copolymers of ethylene and vinyl alcohol, ¹³C NMR investigations have demonstrated the existence of a significant fraction of vinyl alcohol monomer units in the crystallites, whatever the composition of the copolymer.⁸ In contrast, chain defects such as ethyl and butyl branches or acetate branches, present in the same samples, are localized in the amorphous phase only. Besides,

large differences in the crystalline partitioning coefficient related to defects of similar size have been reported. In ethylene/vinyl alcohol random copolymers, P_{CR} values very close to 1 have been obtained for the vinyl alcohol units, whatever the copolymer composition.⁸ This result may suggest that no global energetic penalty results from the replacement of a proton by a hydroxyl group. In contrast, replacing the methyl group of a propylene monomer unit by a proton seems to imply higher energetic costs, since P_{CR} values of 0.42 have been measured on ethylene units of random propylene–ethylene copolymers, the ethylene molar fraction ranging from 0.8 to 7.5 mol %.⁵ Of course, great care has to be taken for a more detailed interpretation of such differences. In particular, additional factors like the crystallization process applied to the samples investigated should be considered since they can affect the P_{CR} value related to a given defect.^{8,11} Last, for a given defect, the dependence of the crystalline partitioning coefficient on the overall defect concentration within the sample varies significantly from one copolymer to another. P_{CR} values related to ethylene in random copolymers of propylene and ethylene remain constant for ethylene content ranging from 0.8 to 7.5 mol %.⁵ The same conclusions hold for the vinyl alcohol units of ethylene/vinyl alcohol copolymers, with vinyl alcohol contents covering a wide concentration range (10–68 mol %).⁸ However, in other copolymers, the insertion of comonomer units in the crystalline phase seems to be easier as soon as a high quantity of the same comonomer has already been incorporated in the crystal lattice. This is the case of poly(β -hydroxybutyrate-co- β -hydroxyvalerate) copolymers: the P_{CR} values related to hydroxyvalerate units tend to increase as their overall concentration in the copolymer is raised.⁹ Therefore, on the basis of these experimental results, it is clear that the cocrystallization of a comonomer is a rather complex phenomenon, and the localization of a given comonomer within the corresponding semicrystalline copolymer cannot be easily predicted.

The aim of this work is to investigate the localization of tetramethylene oxide units introduced along POM chains in order to improve their thermal stability. More precisely, we will consider copolymers based on 1,3,5-trioxane (TOX) and 1,3-dioxepane (DXP) (Table 1), with DXP weight fractions ranging from 3 to 30 wt %. The effect of the tetramethylene oxide units (T units) on the solid-state organization of these copolymers will be first investigated by means of the combined use of DSC, WAXS, and solid-state NMR. In a second step, we will take advantage of the selectivity of solid-state NMR to localize the tetramethylene oxide units within the semicrystalline structures formed by the TOX/DXP copolymers. To our knowledge, the localization of such repeat units in POM-based copolymers has never been studied. This is a first step toward a better knowledge of the correlations between the chemical structure, the solid-state organization, and the mechanical properties of such copolymers. It is also worth remarking that cyclic acetal

Table 2. Composition of the TOX/DXP Copolymers Considered in This Work

sample	ϕ^a (wt %)	φ^b (mol %)	IP ^c (s)
TOX/DXP(97/03)	3	0.9	35
TOX/DXP(90/10)	10	3.1	75
TOX/DXP(80/20)	20	6.4	>225
TOX/DXP(70/30)	30	10.1	>225

^a Weight fraction of dioxepane (DXP) in the TOX/DXP copolymer.^b Molar fraction of tetramethylene oxide (T) units in the copolymer.^c Induction period measured during the copolymerization.**Table 3. Assignment of the ¹³C Resonances in the TOX/DXP Copolymers**

δ^a (ppm)	assignment	f^b (mol %)
25.8	T, $-\text{OCH}_2\text{CH}_2\text{CH}_2\text{CH}_2\text{O}-$	
68.7	T, $-\text{OCH}_2\text{CH}_2\text{CH}_2\text{CH}_2\text{O}-$	
89.3	T(MO)(MO)(MO)(MO)	10.7
89.7	(MO)(MO)(MO)(MO)(MO)	74.1
91.9	(MO)T(MO)(MO)T + T(MO)(MO)T(MO)	1.8
92.5	(MO)T(MO)(MO)(MO) + (MO)(MO)(MO)T(MO)	12.5
94.9	(MO)T(MO)T(MO)	0.9

^a The positions of the ¹³C lines are expressed in ppm with respect to TMS. ^b These molar fractions are determined by integration of the different ¹³C resonances related to the carbon of the MO units within the TOX/DXP(80/20) copolymer.

comonomers like ethylene oxide, 1,3-dioxolane, or 1,3-dioxepane constitute an interesting class of comonomers from a fundamental point of view. Indeed, in contrast with the comonomers or the defects considered until now,^{5,8–10} these comonomers do not introduce any branching along the main chain: the linear architecture of the POM chains is maintained, and only the local chemical structure of the main chain is modified by the insertion of the DXP comonomers. This important feature should play a relevant role in the mechanisms governing the partitioning of the tetramethylene oxide units between the crystalline and amorphous phases of the TOX/DXP copolymers.

2. Experimental Section

2.1. Copolymer Synthesis and Characterization. The copolymers considered in this work were synthesized by cationic copolymerization of molten 1,3,5-trioxane (TOX; BASF) and 1,3-dioxepane (DXP; BASF) in the requisite ratio, at 80 °C, using a catalyst solution of perchloric acid in triethylene glycol dimethyl ether. Further details concerning the synthesis will be reported in a separate contribution. The DXP weight fraction ϕ of the different copolymers and the corresponding molar fraction φ of T units—determined by considering that one dioxepane molecule leads to one methylene oxide unit connected to one tetramethylene oxide unit in the copolymer—are indicated in Table 2. The time at which crystallization occurs during the copolymerization was noted down as the induction period (IP) and reported in Table 2.

The microstructure of the TOX/DXP copolymers was characterized by means of ¹H and ¹³C NMR experiments in solution. The different ¹³C resonances observed on the ¹³C{¹H} NMR spectra and their assignment are listed in Table 3. The distribution of the different pentad sequences centered around a methylene oxide unit (MO unit) is also given in this table, in the case of the TOX/DXP-(80/20) copolymer.

2.2. Solid-State NMR Experiments. Solid-state NMR experiments were performed at room temperature on a Bruker Avance DSX 300 NMR spectrometer operating at a ¹³C Larmor frequency of 75.46 MHz. Low-resolution ¹H NMR experiments were carried out using a 4 mm static Bruker probe, with a ¹H $\pi/2$ pulse length of 3.5 μ s. Spin–lattice relaxation times in the laboratory frame, $T_1(^1\text{H})$, were measured using the inversion–recovery pulse sequence while spin–lattice relaxation times in the rotating frame, $T_{1\rho}(^1\text{H})$,

were determined with a $\pi/2$ spin-lock experiment, the spin-locking field corresponding to 46 kHz. For these ¹H relaxation measurements, the recycle delay was adjusted according to the $T_1(^1\text{H})$ value, thus ranging between 5 and 14 s, depending on the TOX/DXP copolymer considered.

High-resolution ¹³C NMR experiments were performed with a 4 mm magic angle spinning (MAS) double-resonance Bruker probe, at a spinning speed of 5 kHz. ¹³C NMR spectra and ¹³C-detected $T_{1\rho}(^1\text{H})$ measurements were obtained using cross-polarization (CP) experiments, with a ¹H $\pi/2$ pulse length of 4.4 μ s and a proton (carbon) radio-frequency field of 57 kHz during the CP step. The ¹³C NMR signal was detected under high-power proton decoupling (DD, decoupling strength of 80 kHz). For the indirect (via ¹³C) $T_{1\rho}(^1\text{H})$ determinations (delayed CP experiments), the strength of the ¹H spin-locking field was of 57 kHz while the ¹H \rightarrow ¹³C contact time was limited to 100 μ s, in order to prevent ¹H spin-diffusion during the cross-polarization period. For these CP-based experiments, the recycle delay was set between 5 and 14 s, depending on the DXP content of the copolymer. The ¹³C chemical shifts were calibrated with glycine (α -form) as an external reference standard (176.03 ppm for the ¹³C carbonyl signal).

2.3. Wide-Angle X-ray Scattering (WAXS). Wide-angle X-ray powder diffraction data were collected on a D8 Advance Bruker diffractometer in the reflection geometry, using the Cu K α radiation ($\lambda = 0.154$ nm) induced by a generator operating at 40 kV and 40 mA. Diffraction patterns were recorded for 2θ values ranging from 5° to 80°, with an angular increment of 0.05° and a counting time of 4 s per 2θ step.

All the powder diffractograms $I(2\theta)$ were normalized according to their total area A , thus enabling, in a first approach, the comparison between the corresponding diffraction patterns.

2.4. Differential Scanning Calorimetry (DSC). Differential scanning calorimetry experiments were carried out with samples (about 7–9 mg) loaded in aluminum pans on a TA Instruments DSC 2910 calorimeter. Samples were heated at 15 °C min^{−1} from 25 to 200 °C and then cooled to 25 °C with the same rate. The upper temperature after the first heating scan was limited to 200 °C, and the samples were let at this temperature for only 1 min to restrict the POM depolymerization. Despite these attempts to limit the thermally induced sample degradation, the DSC thermograms recorded during the second and third heating (cooling) scans are not identical, for each of the copolymers in the range of DXP content considered. For this reason, in the following, we will only consider the first heating (and cooling) scan obtained on the different copolymers, and therefore, as the thermal history applied to the TOX/DXP samples is not fully controlled when considering the first heating scan, we will restrict our discussion of the DSC data to a qualitative analysis. Besides, at this stage, it is worth noting that all the copolymers have been prepared under similar experimental conditions, at the same period, meaning that the thermal history, even not rigorously the same for the different copolymers, should not differ significantly from one sample to another.

The degree of crystallinity χ_{DSC} of the different TOX/DXP copolymers was estimated by assuming that the heat of melting per unit mass of crystalline material is identical to the heat of melting of a 100% crystalline POM sample (i.e., 317.93 J g^{−1}, according to Iguchi et al.¹²).

3. Results

3.1. Solid-State Organization of the TOX/DXP Copolymers. 3.1.1. Thermal Analysis. Figure 1a depicts the DSC thermograms obtained on the as-synthesized TOX/DXP copolymers, during the first heating and the subsequent cooling scans. A significant decrease of the melting temperature, T_m , of the copolymers is observed as the DXP weight fraction is raised from 3 to 30 wt % (see Figure 1a,b). This result suggests that the insertion of tetramethylene oxide units along the POM homopolymer chains limits the size of the crystallites. In addition, from the cooling response, it can be observed that a

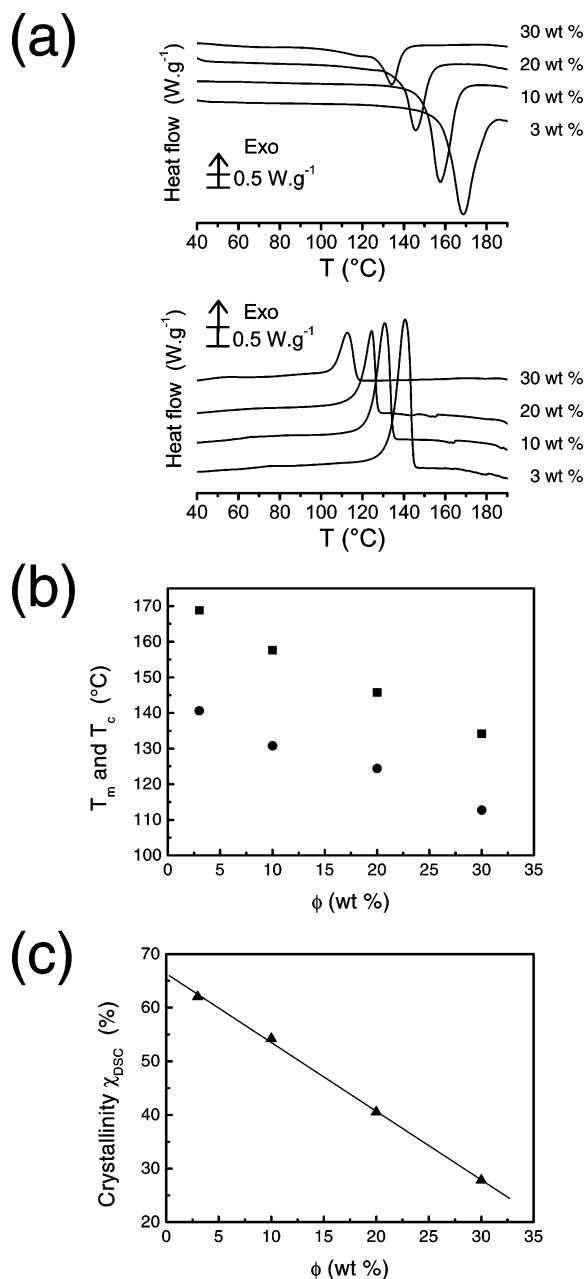


Figure 1. (a) Thermograms recorded on the TOX/DEX copolymers during the first heating scan and the subsequent cooling scan; the heating/cooling rate was set to 15 K min⁻¹. (b) Variation of the melting temperature T_m (■, measured on the first heating scan) and the crystallization temperature T_c (●, measured on the first cooling scan) of the TOX/DEX copolymers, as a function of the DXP weight fraction ϕ . (c) Composition dependence of the crystallinity of the TOX/DEX copolymers, χ_{DSC} , deduced from the melting peak (first heating scan). The line serves as a guide for the eye.

continuous decrease of the crystallization temperature T_c occurs as soon as the DXP content is increased (Figure 1a,b). Therefore, the insertion of tetramethylene oxide units along the POM chains hinders the chain crystallization, and this conclusion is quite consistent with the reduced size of the crystallites, discussed above. Last, the degree of crystallinity χ_{DSC} , deduced from the melting peak observed on the as-synthesized copolymers, is also a decreasing function of the DXP content, as shown in Figure 1a,c. All these observations suggest that the tetramethylene oxide units inserted along the POM homopolymer chains induce a limitation of the crystallization process, and therefore, a decrease of both crystallinity and size of crystallites as the DXP content is increased. These results indicate that a significant

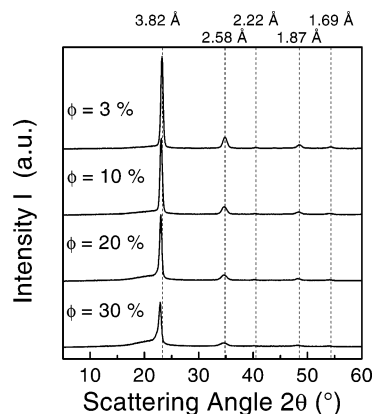


Figure 2. X-ray diffractograms of the TOX/DEX copolymers obtained for dioxepane weight fractions of 3, 10, 20, and 30 wt %. The WAXS data were normalized by the total area under the corresponding diffractogram.

fraction of the tetramethylene oxide units is rejected from the crystalline phase of the TOX/DEX copolymers.

3.1.2. WAXS. More information on the bulk organization of the TOX/DEX copolymers can be obtained using WAXS experiments. The diffraction patterns recorded on the as-synthesized samples are shown in Figure 2. Let us first consider the TOX/DEX copolymer characterized by a DXP amount of 3 wt %. As can be seen in Figure 2, two intense Bragg diffraction peaks can clearly be observed at $2\theta = 23.25^\circ$ and 34.75° , the former being superimposed with the relatively weak contribution of the amorphous halo, located around $2\theta = 21.80^\circ$. This diffraction pattern is very similar to the diffraction pattern of the trigonal form usually observed for the crystalline phase of neat poly(oxymethylene).¹³ In the following, we will describe the crystalline structure using the hexagonal (and not the primitive rhombohedral) cell. The Bragg diffraction peak occurring at $2\theta = 23.25^\circ$ can be assigned to the {100} lattice planes while the peak at $2\theta = 34.75^\circ$ corresponds to the {105} lattice planes.^{14–17} From this indexing, the hexagonal cell parameters related to the crystallites of the TOX/DEX(97/03) copolymer can be derived: $a = b = 4.41$ Å and $c = 17.49$ Å. These cell parameters are very close to the ones reported for neat poly(oxymethylene).^{15–17} Additional Bragg diffraction peaks, although less intense than the ones previously described, can nevertheless be detected at $2\theta = 48.50^\circ$, 54.30° and, to a less extent, 40.55° . They can be assigned to the {115}, {205}, and {111} lattice planes, respectively.

As the overall DXP content is increased from 3 to 30 wt %, the crystalline phase of the TOX/DEX copolymers remains in the hexagonal form, as can be observed in Figure 2. However, the Bragg diffraction peaks are less and less intense while the contribution of the amorphous halo increases as ϕ is raised. One approach to quantify this effect is to estimate the degree of crystallinity χ_{WAXS} from the WAXS patterns. For this purpose, the different Bragg diffraction peaks, as well as the amorphous halo, were fitted by using Gaussian functions. Even though Pearson VII functions are often used to perform this fitting procedure, we have selected, in a first approach, Gaussian-type functions, for the sake of simplicity. A good agreement between the experimental diffractogram and the fitting line was found for all the TOX/DEX copolymers considered. The degree of crystallinity, χ_{WAXS} , can then be estimated as the ratio between the area under the Bragg diffraction peaks over the total area under the crystalline components and the amorphous halo. The variation of χ_{WAXS} with the DXP weight fraction is plotted in Figure 3: the effect of the tetramethylene oxide units is

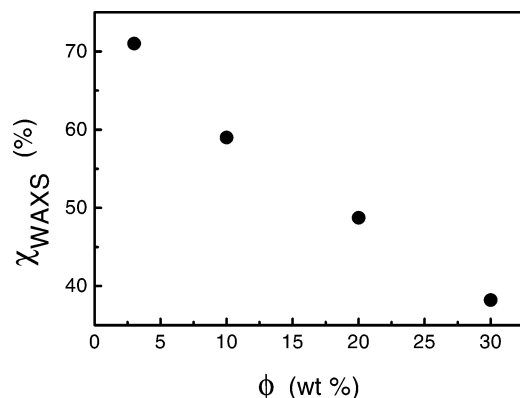


Figure 3. Variation of the crystallinity of the TOX/DEX copolymers deduced from WAXS experiments, χ_{WAXS} , as a function of the overall DXP weight fraction, ϕ .

significant since the crystallinity is reduced by a factor of about 2 as ϕ varies from 3 to 30 wt %. Even though the absolute value of the crystallinity deduced from WAXS and DSC experiments for each of the TOX/DEX copolymers is not exactly the same (χ_{WAXS} being systematically higher than χ_{DSC}), a very good correlation between χ_{WAXS} and χ_{DSC} is observed in the range of DXP content considered. This result confirms the effect of the tetramethylene oxide units on the overall crystallinity, discussed in the previous section.

At this stage of the description of the crystalline domains, it is also of interest to consider the influence of the DXP content on their size. A clear broadening of the Bragg diffraction peaks occurs as soon as the DXP content is increased from 3 to 30 wt % (see Figure 2). This result indicates that the crystallites tend to get smaller. More precisely, an estimation of the apparent crystallite size can be derived from the WAXS data using the Scherrer equation:

$$L_{hkl} = \frac{K\lambda}{\beta_{hkl} \cos \theta_{hkl}} \quad (1)$$

In this equation, β_{hkl} holds for the pure line width of the diffraction peak related to the $\{hkl\}$ lattice planes, located at a scattering angle of $2\theta_{hkl}$. In a first approach, no attempt was made to take into account the instrument broadening, and in the following, β_{hkl} will be replaced by the half-height angular width $\Delta(2\theta_{hkl})$ of the Bragg diffraction peak considered. A value of 0.9 was used for the Scherrer constant K .¹⁸ The L_{hkl} values were derived from the diffraction peak related to the $\{105\}$ crystallographic planes, and the dependence of L_{105} on the overall DXP content is reported in Figure 4. The observed decrease of the degree of crystallinity and the apparent crystallite size while increasing ϕ is somehow expected since the tetramethylene oxide units inserted along the poly(oxyethylene) chains should act as microstructural defects, which disturb the chain regularity and therefore limit the extent of crystallization. Besides, using a 1D two-phase model to describe the semicrystalline organization of the TOX/DEX copolymers, the typical size of the amorphous regions, L_a , can be related to the crystallite size L_c according to the equation $L_c(\chi^{-1} - 1)$. Using for L_c and χ the values of L_{105} and χ_{WAXS} determined by WAXS measurements, the characteristic length L_a is found to increase from 3.6 to 8.9 nm as the DXP content is raised from 3 to 30 wt %. Because of the existence of the constrained amorphous phase, these values should be considered as upper limits of L_a .

More surprisingly, as can be seen in Figure 2, a shift of the 100 reflection toward low angle values is observed when the overall DXP content is raised from 3 to 30 wt %. This feature

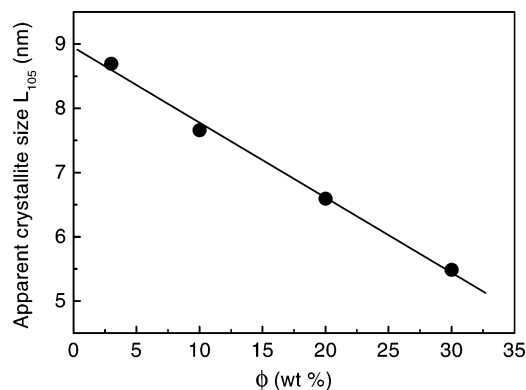


Figure 4. Influence of the DXP content of the TOX/DEX copolymers on the apparent crystallite size, L_{hkl} , estimated with the Bragg diffraction peak related to the $\{105\}$ crystallographic planes using the Scherrer equation.

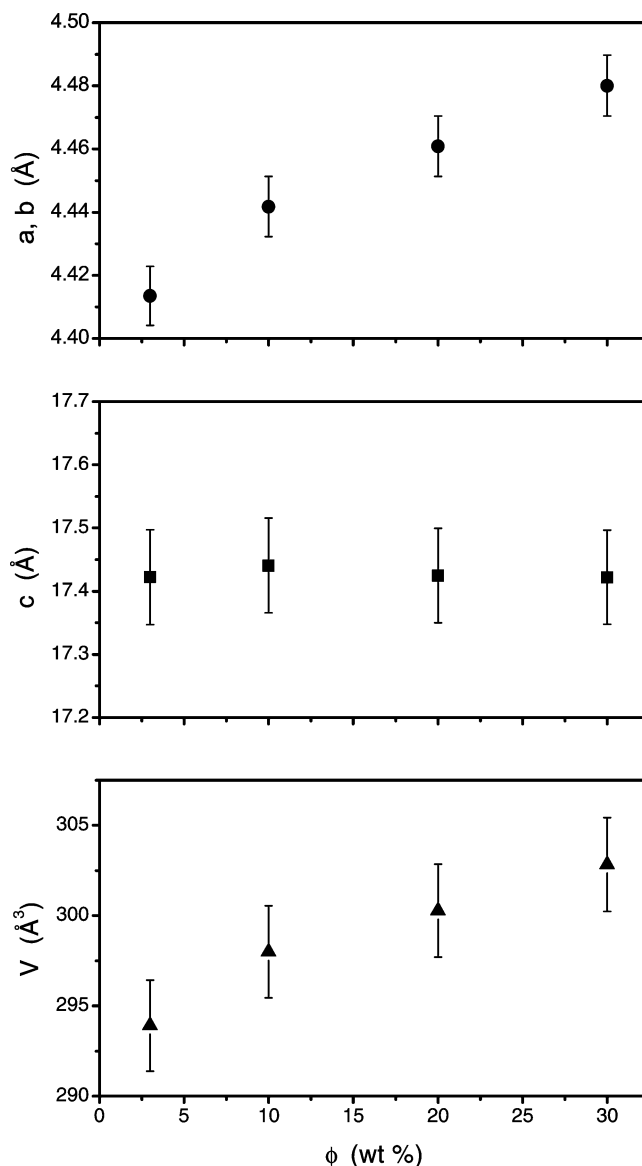


Figure 5. Evolution with the copolymer composition of (a) the a -axis length, (b) the c -axis length, and (c) the volume V of the trigonal cell related to the trigonal form of the TOX/DEX systems.

indicates that the a (and b) parameters of the trigonal cell are increased by the insertion of tetramethylene oxide units along the poly(oxyethylene) chains (see Figure 5). It has to be remarked that this variation of a (and b) as a function of the

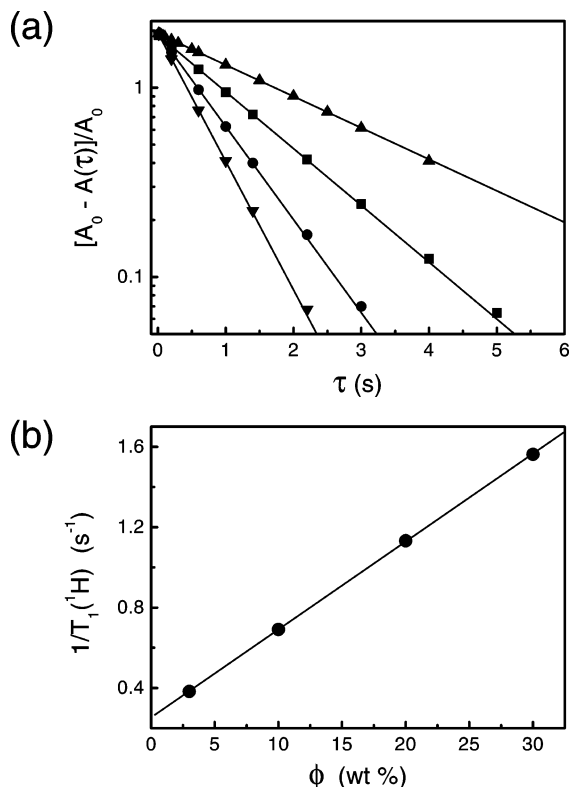


Figure 6. (a) Proton spin–lattice relaxation in the laboratory frame, measured at room temperature on the TOX/DXP copolymers, characterized by different dioxepane weight contents: $\phi = 3$ (▲), 10 (■), 20 (●), and 30 wt % (▼). $A(\tau)$ holds for the amplitude of the proton magnetization following the inversion–recovery experiment, with τ as $T_1(^1H)$ relaxation delay; A_0 stands for the proton magnetization at full equilibrium, under the static NMR magnetic field H_0 . The solid lines represent the linear fits for the different series of data. (b) Composition dependence of the corresponding proton spin–lattice relaxation time in the laboratory frame, $T_1(^1H)$.

copolymer composition ϕ goes beyond the error bars on this parameter. In contrast, the crystallographic parameter c , deduced from the 105 reflection, is found to be nearly unchanged, within the error bars, as the DXP content varies, thus implying that the cell volume V is increased by the introduction of tetramethylene oxide units.

3.1.3. Static 1H NMR Relaxation Measurements. Complementary information about the bulk organization displayed by the TOX/DXP copolymers in the solid state can be derived from proton relaxation measurements. These experiments were carried out on the same samples as the ones used for DSC and WAXS investigations. Figure 6a shows the results of the 1H spin–lattice relaxation time, $T_1(^1H)$, experiments performed on the different TOX/DXP systems. The quantity $A(\tau)$ holds for the amplitude of the 1H magnetization following the inversion–recovery experiment, when selecting τ as the relaxation delay, and A_0 stands for the equilibrium value of the 1H magnetization ($A_0 = A(\tau \gg T_1)$). For each copolymer, the variation of the relaxation signal $[A_0 - A(\tau)]/A_0$ with the recovery time τ can be described by a single-exponential decay: this feature indicates that the magnetization related to amorphous domains and the one related to crystallites equilibrate by 1H spin-diffusion over the $T_1(^1H)$ time scale. In other words, the typical size of both amorphous and crystalline domains is smaller than the 1H spin-diffusion length scale l involved in these $T_1(^1H)$ experiments. l can be estimated using the following equation:

$$l = [6DT_1(^1H)]^{1/2} \quad (2)$$

where D stands for the spin-diffusion coefficient. An upper limit for the value can be obtained using the spin-diffusion coefficient related to the crystalline phase of the copolymers. To our knowledge, no data concerning the spin-diffusion coefficient of both crystalline and amorphous phases of POM have been reported. A rough but reasonable approach consists in considering the spin-diffusion coefficient determined on poly(ethylene oxide): $D_C \approx 0.28 \text{ nm}^2 \text{ ms}^{-1}$ for the crystalline phase and $D_A \approx 0.15 \text{ nm}^2 \text{ ms}^{-1}$ for the amorphous phase.¹⁹ Then, in the TOX/DXP copolymers, amorphous domains as well as crystallites are estimated to be smaller than about 30–70 nm.

The dependence of the $T_1(^1H)$ relaxation time on the DXP weight fraction used for the copolymerization reactions is reported in Figure 6b. As can be seen, the introduction of tetramethylene oxide units induces a strong decrease of the $T_1(^1H)$ value, and more precisely, the variation of the relaxation rate $[1/T_1(^1H)]$ as a function of ϕ is linear over the composition range considered. The observed decrease of the $T_1(^1H)$ value with the DXP content is qualitatively consistent with the reduction of the crystallinity of the TOX/DXP copolymers. If full equilibration of the 1H magnetization due to 1H spin-diffusion between both amorphous and crystalline phases over the $T_1(^1H)$ time scale occurs, then the corresponding relaxation rate $[1/T_1(^1H)]$ can be expressed as a function of the intrinsic $[1/T_1(^1H)]$ values of the amorphous (A) and crystalline (C) regions:

$$[1/T_1(^1H)] = f_A[1/T_1(^1H)]_A + f_C[1/T_1(^1H)]_C \quad (3)$$

f_A and $f_C = 1 - f_A$ hold for the molar fractions of protons contained in the amorphous and crystalline domains, respectively. Considering a series of high-density, linear polyethylene samples, Packer et al. demonstrated that f_C is related to the crystallinity χ by the simple relation

$$f_C = \chi + a \quad (4)$$

with a being a constant.²⁰ According to the DSC or WAXS experiments described in the previous sections, the degree of crystallinity of the TOX/DXP copolymers, either χ_{WAXS} or χ_{DSC} , may be considered as a linear function of the DXP weight fraction, ϕ (see Figure 1c or Figure 3). Therefore, by combining eqs 3 and 4 and the linear variation of χ_{WAXS} or χ_{DSC} with ϕ , one may account for the linear dependence of the relaxation rate $[1/T_1(^1H)]$ with the DXP content, observed in Figure 6b.

It is also of interest to consider the proton spin–lattice relaxation time in the rotating frame, $T_{1\rho}(^1H)$. Indeed, the 1H spin-diffusion length relevant in these $T_{1\rho}(^1H)$ experiments, given by

$$l = 1/2[6DT_{1\rho}(^1H)]^{1/2} \quad (5)$$

is much smaller than the spin-diffusion length involved in $T_1(^1H)$ measurements. Therefore, the $T_{1\rho}(^1H)$ relaxation time is a way to probe the bulk organization displayed by the TOX/DXP copolymers at a lower length scale. The spin–lattice relaxation data in the rotating frame for the protons of the TOX/DXP systems are plotted in Figure 7. Here, the quantity $A(\tau)$ denotes the amplitude of the 1H magnetization following the spin-lock experiment, with τ as the spin-lock time, while A_0 corresponds to the 1H magnetization at equilibrium. Clearly, for all these samples, the variation of A/A_0 as a function of the 1H spin-lock time, τ , displays a significant deviation from a monoexponential behavior. For DXP weight fractions ranging from 3 to 30 wt %, the $T_{1\rho}(^1H)$ relaxation signal can satisfactorily be fitted by

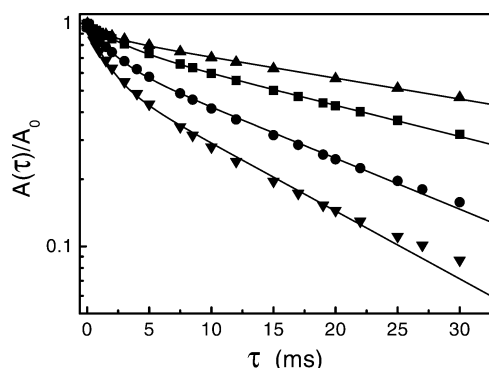


Figure 7. Proton spin–lattice relaxation in the rotating frame, observed at room temperature on the TOX/DXP copolymers related to a dioxepane content of $\phi = 3$ (▲), 10 (■), 20 (●), and 30 wt % (▼). $A(\tau)$ corresponds to the amplitude of the proton magnetization after the 90° spin-lock experiment, τ holding for the spin-locking duration. The data $A(\tau)$ were normalized by A_0 , the proton magnetization at equilibrium. The solid lines stand for the fits of the experimental data by the sum of two monoexponential components.

using two exponential components. The values of the short apparent $T_{1\rho}({}^1\text{H})$ component range from 1.5 to 2.9 ms, while the $T_{1\rho}({}^1\text{H})$ related to the long apparent component varies from 14.3 to 46.3 ms. The deviation from a monoexponential $T_{1\rho}({}^1\text{H})$ relaxation function observed for each of the TOX/DXP copolymers implies that the ${}^1\text{H}$ magnetizations related to the crystallites and to the amorphous regions do not fully equilibrate by ${}^1\text{H}$ spin-diffusion over the time scale given by the shorter $T_{1\rho}({}^1\text{H})$ value.

Depending on the intrinsic $T_{1\rho}({}^1\text{H})$, the typical domain size, and the spin-diffusion coefficient for both crystalline and amorphous regions, the $T_{1\rho}({}^1\text{H})$ relaxation function may consist in more than two exponential components. As a result, the assignment of the short and long apparent components of the $T_{1\rho}({}^1\text{H})$ relaxation data to morphologically distinct regions of the sample (amorphous and crystalline domains, for instance) is not systematically possible.²¹ Here, for each copolymer, the $T_{1\rho}({}^1\text{H})$ data can satisfactorily be described using two components (Figure 7), and no attempt was done to improve the data fit by adding additional $T_{1\rho}({}^1\text{H})$ components. However, such a result does not necessarily imply that amorphous and crystalline domains can be considered as independently relaxing regions. Moreover, for the TOX/DXP copolymers, a significant difference between the relative amplitude of both apparent $T_{1\rho}({}^1\text{H})$ components and the crystallinity of the TOX/DXP copolymers deduced from DSC or WAXS experiments is observed. In particular, the relative amplitude associated with the longer $T_{1\rho}({}^1\text{H})$ decay is systematically higher than the degree of crystallinity. This result indicates that ${}^1\text{H}$ -driven spin-diffusion cannot be neglected over the apparent $T_{1\rho}({}^1\text{H})$ time scale, and the assumption of independently relaxing domains is not correct in the present case. At this stage, it is worth noting that the ${}^1\text{H}$ spin-diffusion coefficient D_A related to the amorphous phase of the TOX/DXP copolymers should be rather small. An order of magnitude for D_A may be obtained using the line width of the narrow component observed on the ${}^1\text{H}$ NMR spectra. With a typical half-height line width of 240 Hz measured on the ${}^1\text{H}$ NMR MAS spectra recorded at a spinning speed of 5 kHz and using the method proposed by Mellinger et al.,²² D_A was estimated to $0.18 \text{ nm}^2 \text{ ms}^{-1}$. Even though this value should be considered as a rough estimate since the ${}^1\text{H}$ half-height line width, instead of the $T_2({}^1\text{H})$ value of the amorphous phase, was used, it indicates that the ${}^1\text{H}$ spin-diffusion length involved in the amorphous domains over the apparent $T_{1\rho}({}^1\text{H})$ time scale should be rather limited. However, although the spin-diffusion

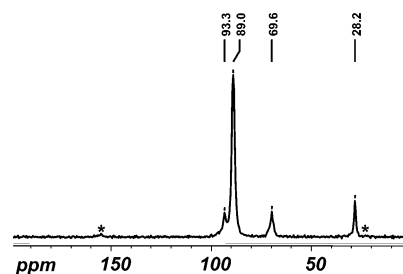


Figure 8. ${}^{13}\text{C}$ CP/MAS/DD spectrum of the TOX/DXP copolymer characterized by a DXP content of 20 wt %. The contact time was set to 1 ms and the spinning speed to 5 kHz. The asterisks stand for the first-order spinning sidebands related to the resonance occurring at 89.0 ppm, these sidebands being of rather low intensity.

coefficient D_A of the amorphous phase is relatively small, the small size of both crystalline (Figure 4) and amorphous regions (see section 3.1.2) should favor the influence of ${}^1\text{H}$ -driven spin-diffusion on the $T_{1\rho}({}^1\text{H})$ relaxation data. Therefore, because of ${}^1\text{H}$ spin-diffusion, there is not an exact correspondence between the protons involved in both apparent $T_{1\rho}({}^1\text{H})$ components and the protons located in crystalline/amorphous domains.

Even though the amplitude of these two apparent $T_{1\rho}({}^1\text{H})$ components cannot be used to get an absolute quantification of the protons involved in both amorphous and crystalline phases of the TOX/DXP copolymers,²¹ it is of interest to note that the amplitude of the faster apparent $T_{1\rho}({}^1\text{H})$ component increases from 10% to 41% as soon as the DXP content is raised from 3 to 30 wt %. Since the crystallinity decreases with the DXP content (see Figures 1c and 3), this feature may suggest that the fast (long) apparent $T_{1\rho}({}^1\text{H})$ component is associated with a dominant amount of amorphous (crystalline) domains. This result is in agreement with the assignment of both $T_{1\rho}({}^1\text{H})$ components in neat poly(oxymethylene), proposed by Veeman et al.²³ At this stage, it is interesting to consider the relatively small value of the short apparent $T_{1\rho}({}^1\text{H})$ (1.5 to 2.9 ms, depending on the TOX/DXP copolymer) in terms of motional processes in the amorphous phase. These motions are fast enough to average the ${}^1\text{H}$ – ${}^1\text{H}$ dipolar interactions to about a few hundred hertz, as evidenced by the line width of the narrow component observed on the ${}^1\text{H}$ MAS NMR spectrum of the copolymers, recorded at a spinning speed of 5 kHz. Moreover, at room temperature (i.e., more than 50°C above the glass transition temperature of the copolymers), the segmental motions in the amorphous phase should exhibit frequencies much higher than the upper-kilohertz region. Thus, the contribution from the α -relaxation process should be rather small in the upper-kilohertz range, at room temperature, and $T_{1\rho}({}^1\text{H})$ should be rather long in the amorphous phase. Therefore, the short apparent $T_{1\rho}({}^1\text{H})$ value is very likely associated with the constrained amorphous or interfacial regions of the copolymers.

Last, the protons involved in the long apparent $T_{1\rho}({}^1\text{H})$ value detected on the TOX/DXP copolymers for instance are not necessarily restricted to the protons of the monomer units forming the crystallites, even though these protons should be dominant. Protons from the constrained amorphous phase and, to a lower extent, protons from the amorphous phase and located in the direct vicinity of the constrained amorphous regions may also be involved in the long apparent $T_{1\rho}({}^1\text{H})$ component.

3.2. Localization of the Tetramethylene Oxide Units within the Semicrystalline Copolymers. 3.2.1. ${}^{13}\text{C}$ CP/MAS/DD NMR Spectra of the TOX/DXP Copolymers. Figure 8 shows the ${}^{13}\text{C}$ CP/MAS/DD NMR spectrum of the TOX/DXP(80/20) copolymer. The ${}^1\text{H} \rightarrow {}^{13}\text{C}$ CP contact time used for this experiment is of 1 ms. Four peaks can be observed in this spectrum.

The line at 89.0 ppm, also present in the ^{13}C NMR spectrum of neat poly(oxyethylene), arises from the carbon of the $-\text{O}-\text{CH}_2-$ units that are directly connected to other $-\text{O}-\text{CH}_2-$ units ((MO)(MO)(MO) sequences). In the solid state of neat poly(oxyethylene),²⁴ this resonance line consists of two overlapping contributions: one located at 89.0 ppm, related to the methylene carbons of (MO)(MO)(MO) sequences involved in the crystalline domains; one occurring about 1 ppm downfield, attributed to the methylene carbons of (MO)(MO)(MO) sequences located in the amorphous domains. However, these two lines strongly overlap and are hardly distinguishable. They have been observed by using techniques that accentuate the spectral contribution of the amorphous phase, such as the use of a $T_2-(^1\text{H})$ filter.²⁴ In the ^{13}C NMR spectrum of the TOX/DXP(80/20) copolymer, the half-height line width of the ^{13}C NMR peak related to the MO units of the (MO)(MO)(MO) sequences involved in the crystallites is of the order of 2 ppm. As a result, the two contributions associated with the amorphous and crystalline domains and separated by 1 ppm are not discernible. This is also the case for all the other TOX/DXP copolymers considered in this study.

A first feature that may explain the difficulties to clearly observe the signature of the MO units in the amorphous phase on the ^{13}C CP/MAS/DD spectra is the high propensity of these units to form crystalline domains, thus minimizing the contribution from the noncrystalline regions. However, as the DXP content is raised to 30 wt %, the significant reduction of the crystallinity does not permit to observe a clear contribution of the MO units located in the amorphous phase. This result indicates that additional features may be responsible for the difficulties to detect the amorphous MO units: the rather low $^1\text{H} \rightarrow ^{13}\text{C}$ CP transfer efficiency (in contrast with the crystalline regions), induced by the high segmental mobility within the amorphous phase at room temperature, combined with the lower intrinsic $T_{1\rho}(^1\text{H})$ value of the amorphous phase (compared to the longer $T_{1\rho}(^1\text{H})$ of the crystallites). Moreover, in the case of the TOX/DXP copolymers, a ^{13}C NMR resonance occurring at 93.3 ppm makes the observation of the MO units of the (MO)(MO)(MO) sequences located in the amorphous phase more difficult as ϕ increases. This resonance at 93.3 ppm can be assigned to the carbons of methylene oxide units connected, at least, to one tetramethylene oxide monomer unit. This assignment is based on the distribution of pentad sequences centered around a MO unit, as probed on the same copolymer, by ^{13}C NMR experiments in solution (see Table 3).

The peaks occurring at 69.6 and 28.2 ppm in Figure 8 are assigned to the α - and β -methylene carbons of the tetramethylene oxide monomer units, respectively. These values are quite close to the chemical shifts of neat poly(tetramethylene oxide) (PTMO): Hirai et al.²⁵ measured ^{13}C chemical shifts for PTMO at 273 K, equal to 72.9 ppm (70.9 ppm) and to 28.3 ppm (27.0 ppm) for α - and β -methylene carbons involved in the crystalline (amorphous) domains of semicrystalline PTMO. Schmidt et al.²⁶ reported similar values for the PTMO blocks of poly(butylene terephthalate)/PTMO block copolymers at room temperature: 72.5 ppm (71.0 ppm) for the α -methylene carbons in crystalline (amorphous) domains, while the resonance of the β -methylene carbons, which overlaps with the line related to the internal methylene groups of the poly(butylene terephthalate) blocks, was located at 27.5 ppm.

The comparison of the ^{13}C chemical shift values related to the T units of the TOX/DXP copolymers could be a straightforward way to determine whether some of these units are inserted within the crystalline phase or are located in the

amorphous phase only. However, PTMO crystallizes in the all-trans, planar zigzag conformation^{27,28} while in neat POM, polymer chains display the 9_5 helical conformation.^{14–16} Therefore, if T units are inserted within the crystalline domains, their conformation may differ from the all-trans one. Then, the ^{13}C chemical shift of the resonances related to PTMO crystalline domains may not be the proper reference to interpret the ^{13}C chemical shift values of the T units in the TOX/DXP copolymers in terms of location of these units within the crystalline phase. In addition, each T unit is necessarily connected to one MO unit, and this feature should affect the ^{13}C chemical shift values of the T units, whatever their location within the crystalline or amorphous regions. For all these reasons, the ^{13}C chemical shift measured on the T units of the TOX/DXP copolymers cannot be used to determine whether some of these units can be inserted within the crystalline domains. The same conclusions hold for the MO units directly connected to T units (^{13}C NMR peak occurring at 93.3 ppm). Consequently, in the following, ^{13}C -detected ^1H spin-lattice relaxation time in the rotating frame ($T_{1\rho}(^1\text{H})$) measurements will be carried out to probe the location of the T units within the semicrystalline organization displayed by the TOX/DXP copolymers.

3.2.2. ^{13}C -Detected $T_{1\rho}(^1\text{H})$ Measurements. The ^{13}C -detected $T_{1\rho}(^1\text{H})$ determinations take advantage of the contrast between the carbons related to methylene oxide and tetramethylene oxide monomer units, in terms of ^{13}C chemical shifts. In these experiments, a contact time of 100 μs was used for the $^1\text{H} \rightarrow ^{13}\text{C}$ cross-polarization step. The variation of the integral A of the ^{13}C NMR peak at 89.0, 69.6, and 28.2 ppm with the proton spin-lock time, τ , is shown in Figure 9. In the case of the resonance at 89.0 ppm, the area was calculated between 76.0 and 107.0 ppm, thus including the contribution from the peak at 93.3 ppm. Whatever the resonance considered, the $T_{1\rho}(^1\text{H})$ decay is not monoexponential. It can be described in terms of a sum of two monoexponential functions with $T_{1\rho}(^1\text{H})$ values of the order of 2–3 and 21 ms, very close to the $T_{1\rho}(^1\text{H})$ values determined from the direct $T_{1\rho}(^1\text{H})$ experiments.

As can be seen in Figure 9b,c, the $T_{1\rho}(^1\text{H})$ relaxation curves determined on the integral of the ^{13}C resonances at 69.6 and 28.2 ppm, related to the outer and inner methylene carbons of the T units, respectively, are nearly superposable, as expected since the two carbon types belong to the same T units. In contrast, the $T_{1\rho}(^1\text{H})$ decay of the 89.0 ppm line differs from the $T_{1\rho}(^1\text{H})$ decays observed for the two other lines. The $T_{1\rho}(^1\text{H})$ values are identical for the three lines, but the relative amplitude of the shorter apparent $T_{1\rho}(^1\text{H})$ component, associated with the intrinsic $T_{1\rho}(^1\text{H})$ of the amorphous phase, is much higher for the T units than for the MO units (53% for the T units, against 18% for the MO units).

Let us first remark that the resonance at 93.3 ppm should contribute to the short apparent $T_{1\rho}(^1\text{H})$ component observed in Figure 9a. However, this contribution is rather weak: the corresponding area, estimated on the ^{13}C -detected $T_{1\rho}(^1\text{H})$ measurements recorded with a ^1H spin-lock duration of 20 μs , represents about 6% of the total area A between 76.0 and 107.0 ppm. A similar value was obtained using a deconvolution procedure and a “cut and weight” method. As a result, the integral of the ^{13}C peak at 93.3 ppm is not high enough to account for the relative amplitude related to the faster $T_{1\rho}(^1\text{H})$, which is of about 18% (Figure 9a). The remaining contribution to the short apparent $T_{1\rho}(^1\text{H})$ component should include central methylenes in (MO)(MO)(MO) sequences.

A first feature that may rationalize the difference between the behavior of the MO and T units is the differences in the

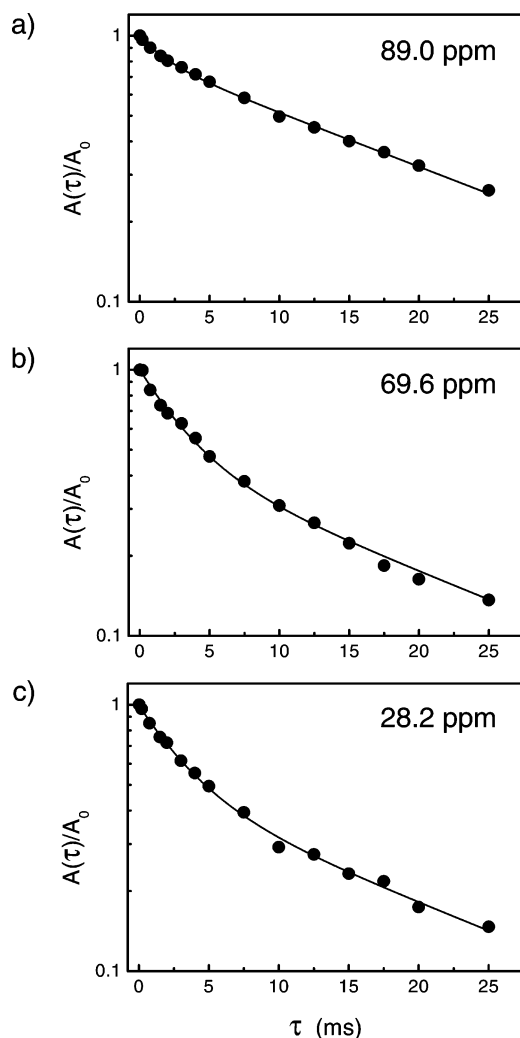


Figure 9. ^{13}C -detected ^1H spin-lattice relaxation in the rotating frame obtained on the different ^{13}C NMR peaks of the TOX/DXP(80/20) copolymer: (a) resonance at 89.0 ppm (carbons of methylene oxide units directly connected to other $-\text{CH}_2-\text{O}-$ units); (b) and (c) resonances at 69.6 and 28.2 ppm (α - and β -methylene carbons of the tetramethylene oxide units). $A(\tau)$ stands for the ^{13}C peak integral obtained with τ as a ^1H spin-lock duration and $A_0 = A(\tau = 0 \text{ ms})$. For these experiments, the contact time used for the $^1\text{H} \rightarrow ^{13}\text{C}$ cross-polarization step was set to 100 μs .

partitioning behavior between the T and MO units within the semicrystalline TOX/DXP(80/20) copolymer. Indeed, acting as microstructural defects along the POM chains, a significant part of the T units should be located in both amorphous and interfacial regions, and this fraction should be at least larger than the one related to the MO units, which display a high tendency to participate to crystalline regions, when involved in sufficiently long (MO)(MO)...(MO)(MO) sequences. As a result, even though there is not a direct correlation between the different apparent $T_{1\rho}(^1\text{H})$ components and the morphologically distinct regions of the TOX/DXP(80/20) copolymer, the difference in the partitioning of the T and MO units may give rise to a higher relative amplitude of the shorter $T_{1\rho}(^1\text{H})$, close to the intrinsic $T_{1\rho}(^1\text{H})$ of the amorphous phase.

Another feature may also account for the higher relative amplitude of the faster apparent $T_{1\rho}(^1\text{H})$ component observed on the T units. In these random copolymers, the T units are quite isolated along the copolymer chains, as demonstrated by ^{13}C NMR experiments in solution (see Table 3), and at room temperature (i.e., well above the glass-transition temperature of the amorphous phase of the copolymer), the segmental

mobility should be nearly identical for both kinds of units, resulting in similar $^1\text{H}-^{13}\text{C}$ dipolar couplings. Therefore, under these conditions, the $^1\text{H} \rightarrow ^{13}\text{C}$ cross-polarization efficiency for the carbons of MO and T units in the amorphous phase should be very similar, and the same remark is valid for the constrained amorphous phase. Even though these units share the same segmental mobility, variations in these dipolar couplings may be induced by the differences in the local chemical structure of each carbon type: two oxygen atoms for the MO unit carbons, one oxygen atom and one methylene group for the α -methylene carbons of the T units, and two methylene groups for the β -methylene carbons of the T units. However, the ^{13}C CP/MAS/DD NMR spectra recorded on the TOX/DXP(80/20) copolymer for contact times ranging between 20 μs and 8 ms display identical area for both resonances of the T units. Thus, these observations tend to demonstrate that the occurrence of one or two methylene group(s) as direct neighbors along the chains does not lead to detectable differences in the averaged $^1\text{H}-^{13}\text{C}$ dipolar couplings of both types of T unit carbons. One may reasonably extrapolate this result to the MO unit carbons, surrounded by two oxygen atoms. Under this assumption, if the T and MO units exhibited identical concentration profiles in the amorphous phase, the $T_{1\rho}(^1\text{H})$ relaxation curves determined using the integrals of the resonances occurring at 28.2, 69.6, and 89.0 ppm should be similar. This is not the behavior observed experimentally, which may suggest that the concentration profile for the T units in both amorphous and interfacial regions should differ from the one of the MO units. In particular, one may suggest that the concentration of T units progressively increases going from the amorphous phase toward the constrained amorphous regions. As the segmental dynamics is slowed down from the amorphous phase toward the interfacial regions, an increase of the corresponding $^1\text{H}-^{13}\text{C}$ dipolar couplings, and thus of the $^1\text{H} \rightarrow ^{13}\text{C}$ cross-polarization efficiency, should occur. If the spatial distribution of the T units displays a progressive increase from the amorphous zones toward the interfacial regions, the global ^{13}C contribution from the T units located in both amorphous and constrained amorphous phases will be higher than the one of the MO units. This feature is in agreement with the higher relative amplitude of the faster $T_{1\rho}(^1\text{H})$ component observed on the T units. Besides, the ^1H -driven spin-diffusion process leads to a varying amplitude of the longer apparent $T_{1\rho}(^1\text{H})$ component within the semicrystalline morphology. This ^1H relative polarization should decrease from the crystalline regions toward the amorphous domains, with intermediate values in the interfacial zones. Thus, if the T units are clustered in the interfacial regions, the corresponding apparent fraction of the faster $T_{1\rho}(^1\text{H})$ component will be larger than the one related to the MO units. In this respect, the differences in the amplitude of the faster $T_{1\rho}(^1\text{H})$ component observed in Figure 9 would be compatible with a location of the T units at the interface between crystalline and noncrystalline regions.

From another point of view, Figure 9b,c shows that the T units also contribute to the longer apparent $T_{1\rho}(^1\text{H})$ component. Here, it is important to remind that the protons involved in the long apparent $T_{1\rho}(^1\text{H})$ component are not restricted to the ones located in the crystalline regions. Because of ^1H -driven spin-diffusion, the protons of the chain segments constituting the constrained amorphous phase and some protons from the amorphous phase, just in the vicinity of the constrained amorphous domains, should also be considered as contributing to the longer apparent $T_{1\rho}(^1\text{H})$ component. For this reason, the occurrence of the long apparent $T_{1\rho}(^1\text{H})$ component on the $T_{1\rho}$ -

(^1H) relaxation curves reported in Figure 9b,c implies that some tetramethylene oxide units are located either in the crystallites of the TOX/DXP(80/20) copolymer or in the constrained amorphous phase surrounding the crystallites. As a first approximation, one may neglect the contribution of the protons of the amorphous phase that could potentially be involved in the long apparent $T_{1\rho}(^1\text{H})$ component. Because of the low $^1\text{H} \rightarrow ^{13}\text{C}$ CP efficiency in the amorphous phase, the ^{13}C contribution at 69.6 and 28.2 ppm due to these protons following the short CP transfer (contact time of 100 μs) is very small. This conclusion is supported by the comparison of ^{13}C CP/MAS/DD NMR spectra of the TOX/DXP(80/20) copolymer recorded for various contact times. No variation in the line shape of the ^{13}C NMR peaks related to the T units is detected as the $^1\text{H} \rightarrow ^{13}\text{C}$ CP contact time is raised from 20 to 100 μs . Consequently, one can confidently consider that a contact time of 100 μs is short enough to neglect the response from the T units in the amorphous domains on the ^{13}C NMR spectra of the TOX/DXP(80/20) copolymer.

As mentioned above, the ^{13}C NMR spectra obtained in a ^{13}C -detected $T_{1\rho}(^1\text{H})$ experiment with a $^1\text{H} \rightarrow ^{13}\text{C}$ CP contact time of 100 μs are dominated by the contribution from both crystalline and interfacial regions. It is worth noting that the ^{13}C line shape related to both T unit resonances remains nearly unchanged as the ^1H spin-lock time τ is raised from 20 μs to 25 ms. Let us first make the assumption that, in addition to the T units located in the interfacial zones, including the crystalline side of the crystalline/noncrystalline interfaces, a significant amount of T units is also incorporated in the crystalline phase. The ^{13}C NMR line shape of the resonances resulting from the T units potentially incorporated in the crystallites is expected to differ from the one of the T units involved in the interfacial zones. Indeed, even though the T units potentially inserted in the crystallographic lattice do not display a POM-like helical conformation but adopt a different conformation, the difference in the interchain packing (and in the conformational behavior) should result in a distinct ^{13}C NMR line for T units in the crystallites and the ones at the interfaces. As a result, in the ^{13}C -detected $T_{1\rho}(^1\text{H})$ experiments, the ^{13}C line shape of the T unit resonances should essentially correspond to a linear combination of the ^{13}C line shape resulting from the interfacial zones and the one related to the T units in the crystallites. Therefore, as the ^1H spin-lock is varied from values small compared to the apparent faster $T_{1\rho}(^1\text{H})$ to values much higher than the faster $T_{1\rho}(^1\text{H})$, a variation in the line shape of the ^{13}C resonances at 69.6 and 28.2 ppm should be observed. This is not the case experimentally, which implies that the total amount of T units in the crystallites must be quite small. Of course, we cannot conclude that all the T units are only restricted to the interfacial regions, and the occurrence of a decreasing gradient of the T unit concentration from the crystallite surfaces toward the inner crystallites cannot be discarded. In contrast, the shape of the ^{13}C resonance at 89.0 ppm gets narrower as soon as the ^1H spin-lock time is increased from 20 μs to 25 ms. Such a change results from the decreasing relative contribution of a relatively wide signal, at the bottom of the ^{13}C line, that may be more easily observed for short ^1H spin-lock times. In particular, this relative decrease can be detected in the downfield side of the ^{13}C NMR peak at 89.0 ppm, which does not display any overlap with another peak, in contrast with the upfield part. This result may be attributed to the contribution of MO units in both interfacial and crystalline regions: as the ^1H spin-lock time increases, the ^{13}C resonance at 89.0 ppm is more and more dominated by the contribution from the MO units located in

the crystalline domains, which display a narrower line shape than the MO unit carbons of the interfacial regions. In addition, this feature validates the assumption that the ^{13}C line shape related to carbons in the interfacial zones should differ from the line shape of carbons in the inner crystalline regions.

An additional observation should be mentioned. Considering the ^{13}C NMR peak related to the carbons of the (MO)(MO)-(MO) sequences involved in the crystalline regions, it is clear that no change in the ^{13}C chemical shift value of this peak (89.0 ppm) is detected when ϕ is increased from 3 to 30 wt %. Similarly, the half-height line width of this peak (about 135 Hz) does not vary with the copolymer composition. These two observations suggest that the helical conformation displayed by the MO units in the crystalline regions is not affected by the incorporation of T units along the copolymer chains. This result is consistent with a preferential location of the T units in the interfacial regions, rather than a uniform spatial distribution within the crystalline domains.

In summary, in the TOX/DXP(80/20) copolymer, a large part of the T units is expected to be located in the amorphous phase. The combination of the different NMR observations previously discussed tends to indicate that the remaining fraction of T units is mostly located in the interfacial regions with the amorphous domains, including the crystalline side of the crystalline/noncrystalline interfaces. Of course, the concentration profile for the T units from the interfacial zones toward the crystallites may display a continuous decrease. However, our experiments indicate that even if some T units may be incorporated in the crystalline domains, these units are far from being dominant.

The ^{13}C -detected $T_{1\rho}(^1\text{H})$ experiments have been carried out for all the other TOX/DXP copolymers, characterized by $\phi = 3, 10$, and 30 wt %. All these copolymers exhibit a behavior which is very close to the case of the TOX/DXP(80/20) copolymer behavior. In this context, one interesting question concerns the concentration of T units in the interfacial and crystalline regions of the TOX/DXP copolymers and its comparison with the overall concentration of T units involved in the copolymer synthesis. In order to obtain a ^{13}C NMR spectrum of both interfacial and crystalline regions, we have used a delayed CP pulse sequence with (i) a very short contact time of 100 μs and (ii) a long ^1H spin-lock time of 10 ms ($\gg [T_{1\rho}(^1\text{H})]_s$, value associated with the intrinsic $T_{1\rho}(^1\text{H})$ of the amorphous domains). Moreover, we have taken advantage of the similar values of the so-called cross-relaxation time constant T_{CH} that should be displayed by the different carbons of both MO and T units located in the interfacial regions (and, similarly, in the crystalline phase). Therefore, the ratio r , defined as

$$r = \frac{0.25[A(28.2 \text{ ppm}) + A(69.6 \text{ ppm})]}{0.25[A(28.2 \text{ ppm}) + A(69.6 \text{ ppm})] + [A(89.0 \text{ ppm}) + A(93.3 \text{ ppm})]} \quad (6)$$

$A(i)$ standing for the area under the ^{13}C NMR resonance line i , may be used to estimate the ratio of the T units over the total number of monomer units (MO or T units), in the crystalline and interfacial phases. The dependence of this parameter r on the overall fraction ϕ of T units within the TOX/DXP copolymers is reported in Figure 10a. Clearly, the concentration of T units in the interfacial regions and in the crystalline phase increases with the fraction of dioxepane introduced during the copolymerization. The propensity for the T units to be inserted at the noncrystalline/crystalline interfaces or within the crystallites of the TOX/DXP copolymers can be quantified using the so-called partitioning coefficient, $P_{\text{CL/CR}}$. In our case, this

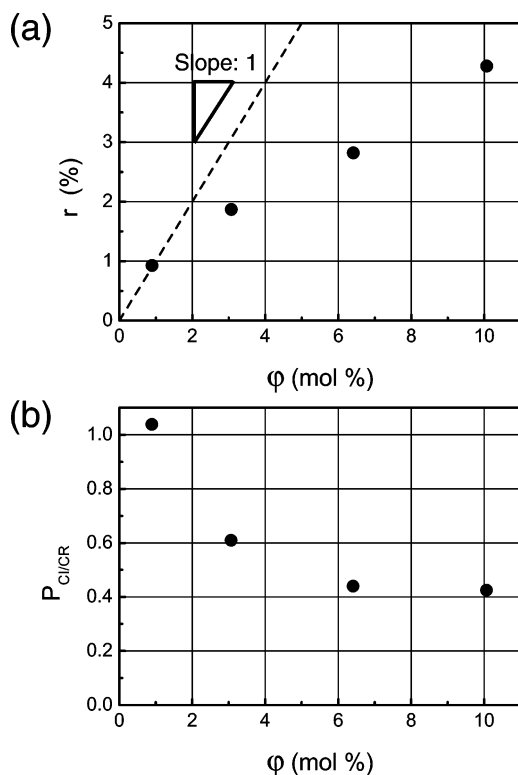


Figure 10. (a) Correlation between the concentration r of tetramethylene oxide (T) units in the interfacial and crystalline regions and the global molar fraction ϕ of T units in the TOX/DXP copolymers. (b) Dependence of the partitioning coefficient $P_{Cr/CI}$ of the T units with the global copolymer composition ϕ .

parameter corresponds to the ratio of the concentration of T units in the crystalline phase and in the surrounding interfacial zones over the concentration of T units in the copolymer. Our solid-state ^{13}C NMR experiments permit to determine the coefficient $P_{Cr/CI}$ ($P_{Cr/CI} = r/\phi$) for each copolymer, and the resulting $P_{Cr/CI}(\phi)$ variation is shown in Figure 10b. The partitioning coefficient $P_{Cr/CI}$ related to the T units is close to 1 in the TOX/DXP(97/03) copolymer, within experimental accuracy. It decreases toward a constant value of 0.40 as soon as the DXP content used for the copolymerization is raised. Therefore, this result indicates that, as the global concentration of T units within the TOX/DXP copolymers increases, their insertion in both interfacial and crystalline phases seems to be more and more difficult, and these units are preferentially localized in the free amorphous phase.

At this stage, it is important to notice that the interpretation of the decreasing behavior of $P_{Cr/CI}(\phi)$ should not be based on thermodynamic arguments only but should also include kinetic considerations since the TOX/DXP copolymers studied in this work may be out of equilibrium. Indeed, in the range of DXP content considered, the copolymer chains crystallize in a few tens of seconds during the synthesis. Therefore, one may imagine that the crystallization process is so fast that a significant amount of T units are “trapped” in the interfacial and crystalline regions. The amount of these “trapped” T units, which is expected to modulate the value of their partitioning coefficient $P_{Cr/CI}$, and its dependence on the DXP weight fraction should depend on the crystallization kinetics of the different copolymers during their synthesis. The difference of crystallization kinetics during the copolymerization is far from being obvious to observe experimentally and cannot be discussed by considering simple parameters as the induction period measured during the copolymer synthesis (Table 2), since as

soon as the DXP content is increased above 10 wt %, a gel formation before crystallization is observed. To discuss the thermodynamic and/or kinetic contributions to the observed composition dependence of $P_{Cr/CI}$ in more detail, it would be useful to probe the influence of the crystallization conditions on the $P_{Cr/CI}(\phi)$ variation. In particular, it would be of interest to carry out the $P_{Cr/CI}$ determination on slowly cooled TOX/DXP copolymers from their molten state. However, for this purpose, the samples have to be heated above 200 °C, left at this temperature for about 10–15 min, and then slowly cooled. According to our DSC experiments, such a procedure leads to a degradation of the samples, which would not necessarily be the same for all the TOX/DXP copolymers, depending on the DXP content.

4. Discussion and Conclusions

The TOX/DXP copolymers considered in this work offer a good avenue to investigate the morphological partitioning of linear units, namely tetramethylene oxide units, acting as structural defects inserted along linear chains of a semicrystalline homopolymer (poly(oxymethylene) chains in this case). This situation differs somehow from the case where the comonomer introduces branches along the main chain.^{5,7–10}

The overall concentration of T units within the copolymers investigated remains quite limited, since it ranges from 0.9 to 10.0 mol %. In addition, the T units should be rather isolated along the copolymer chains. Indeed, a T unit cannot be directly connected to another one, since it would involve a highly unstable carbonium ion, $-\text{O}-\text{CH}_2-\text{CH}_2-\text{CH}_2-\text{CH}_2^+$, as a propagating center during the copolymerization.²⁹ In addition, ^{13}C NMR characterizations of the TOX/DXP copolymers in solution have shown that the contribution of T units separated by only one or two MO units is nearly negligible (see Table 3). As expected, these “isolated” defects induce a significant decrease of both crystallinity and crystallite size in the TOX/DXP copolymers, as the DXP content used during the synthesis is raised. Our solid-state NMR investigations have demonstrated that a fraction of these T units are inserted within the crystallites and/or in the regions at the interface between the crystalline and the amorphous phases. More precisely, in the scheme that emerges from the analysis of the NMR data, the T units tend to concentrate in the interfacial zones, on either the disordered or ordered side of the noncrystalline/crystalline interface. Of course, the occurrence of T units in the interior of the crystallites cannot be discarded, but their amount should be quite low. This limited amount of potential crystallographic defects may explain that, for all the TOX/DXP copolymers considered, the crystallographic lattice remains the same as the one observed in neat poly(oxymethylene), even though neat POM and neat PTMO give rise to different kinds of crystallographic lattices.^{14–17,27,28}

Another interesting feature concerns the variation of the crystallographic cell parameters observed as the overall DXP content of the TOX/DXP copolymers is changed. Indeed, as can be seen in Figure 2, the Bragg diffraction peak occurring at $2\theta = 23.25^\circ$, which can be assigned to the $\{100\}$ lattice planes of the hexagonal lattice, shifts toward low angles as the DXP content in the copolymer is increased above 3 wt %. Even though a broadening of this peak also occurs as ϕ is raised, nearly no diffraction signal remains at the location of the same diffraction peak, measured on the TOX/DXP(97/03) copolymer. This result suggests that the incorporation of T units along the poly(oxymethylene) chains induces a distortion of the crystallographic unit cells forming the copolymer crystallites: no undistorted POM crystallites were detected. The ^{13}C NMR

investigations performed on the TOX/DXP copolymers have shown that a part of the T units are located in the interfacial regions, on the disordered side of the interface (constrained amorphous phase), and/or on the crystalline side (unit cells at the surfaces of the crystallites). In this context, in order to rationalize the expansion of all the crystallographic unit cells, it is important to remark that the crystallites occurring within the TOX/DXP copolymers are rather small: from the WAXS experiments, the apparent crystallite size was found to decrease from 8.7 to 5.5 nm as the DXP content increases from 3 to 30 wt %. This means that the number of crystallographic cells along one direction would be of the order of 3–5 only if the *c*-direction is considered and 12–20 when the *a*-axis is considered. As a result, if a T unit is incorporated in the crystalline side of the noncrystalline/crystalline interfaces, a distortion of the nearest crystallographic cells may occur. Such a distortion may easily propagate through all the crystalline cells due to the rather small crystallite size observed on the TOX/DXP copolymers. Similarly, if the average volume occupied by a T unit is higher than the one related to two or three MO units, the T units that are located in the disordered side of the interfacial regions may also induce constraints on the crystalline cells in their close surrounding and would thus contribute to the expansion of the crystallographic cells forming the crystallites. Last, it is worth noting that our ^{13}C NMR experiments cannot exclude the occurrence of T units in the interior of the crystallites, even though their amount should be much lower than the one in the interfacial regions. Such T units, even not numerous, would also contribute to the deformation of the hexagonal lattice according to the same mechanism as before.

Last, our WAXS measurements demonstrate that the incorporation of T units in the interfacial regions and, to a lower extent, in the interior of the crystallites leads to an increase of the cell volume *V*. However, the parameter *c* does not vary with the molar fraction of T units, in contrast with the lattice parameters *a* and *b*, which increase with φ . The ^{13}C NMR investigations performed in this work do not enable to discriminate unambiguously each side of the noncrystalline/crystalline interfaces. However, in the case of a distortion of the crystallographic lattice mostly induced by the incorporation of T units in the crystallites (either at the surfaces or in the interior of these crystallites), the composition dependence of the lattice parameters *a*, *b*, and *c* may seem, at first glance, rather surprising, taking into account the fact that, in neat poly-(oxymethylene), the chains are organized in 9_5 helices, the axis of which coincides with the *c* direction.^{14–17} Therefore, naively, one could have expected that a T unit inserted within the crystallites would also display a helical conformation around the *c*-axis, thus tending to induce an increase of the *c* parameter, *a* and *b* remaining nearly unchanged. This is not the trend observed when considering the dependence of *a* and *c* with the copolymer composition. One possibility to interpret these WAXS results is to consider that the T units (and maybe the nearest-neighbor MO units along the considered copolymer chains) would display a squeezed conformation, with respect to the *c*-axis, in order to limit the disorder introduced in the helical chain conformation by their insertion in the crystallites. In such a scheme, the incorporation of T units in the crystallographic cells should not strongly affect the value of the parameter *c*, and therefore, the increase of the cell volume *V* induced by the substitution of methylene groups for oxygen atoms should result in the increase of the parameter *a* with the DXP content.

5. Conclusions

Results obtained by solid-state NMR, WAXS, and DSC on a series of TOX/DXP copolymers have shown that a large amount of T units are located in the free amorphous phase. The remaining T units tend to concentrate at the noncrystalline/crystalline interface. These T units can be localized either on the disordered side of the interface, i.e., in the constrained amorphous phase, or on the crystalline side, i.e., in the crystalline cells at the crystallite surfaces. The occurrence of T units in the interior of the crystallites, through a decreasing gradient of concentration from the interfaces toward the inner crystallites for instance, cannot be discarded.

From the point of view of the structure–properties relationship, the copolymerization of 1,3,5-trioxane with 1,3-dioxepane is one of the strategies that has been selected to improve the thermal behavior of neat poly(oxymethylene). The insertion of T units along the chains results in a decrease of both degree of crystallinity and crystallite size and thus in a decrease of the mechanical performances of the corresponding copolymers. In addition, the observed composition dependence of $P_{\text{CL/CR}}$ suggests that the pure amorphous phase will get richer in T units, as the DXP content is increased from 3 to 30 wt %. As the glass-transition temperature, T_g , in neat PTMO is much lower than the one in neat POM, the resulting T_g value of the amorphous phase should decrease as φ is raised, inducing an additional decrease of the mechanical performances of the TOX/DXP copolymers. Thus, the results obtained suggests to use the smallest DXP content compatible with the requirements related to the thermal properties of these materials in order to benefit from the localization of the highest amount of T units in the interfacial and crystalline regions but also to restrict the reduction of the crystallinity. In this respect, it would be interesting to determine the $P_{\text{CL/CR}}(\varphi)$ variation for other types of comonomers, ethylene oxide or 1,3-dioxolane namely. Indeed, with 1,3-dioxolane as a comonomer for instance, the insertion of a trimethylene oxide unit along the POM chains would correspond, at the location of the insertion, to the substitution of a methylene group for one oxygen atom. It should induce a smaller perturbation than the one introduced by T units. Therefore, investigating the influence of the nature of the cyclic acetal comonomer on the $P_{\text{CL/CR}}(\varphi)$ variation would help to go further in the optimization of these POM-based copolymers.

Acknowledgment. The authors acknowledge the fruitful discussions with various colleagues at BASF Research, CNRS-UMR 7581 and CNRS-UMR 7610. C.L. and F.L. gratefully acknowledge CNRS and French Minister of Science for financial support and thank Région Ile-de-France for its participation in the purchase of the solid-state NMR spectrometer. The authors also express their gratitude to Dr. D. L. VanderHart for his constructive and fruitful remarks.

References and Notes

- (1) Schweitzer, C. E.; MacDonald, R. N.; Punderson, J. O. *J. Appl. Polym. Sci.* **1959**, *1*, 158–163.
- (2) Koch, T. A.; Lindvig, P. E. *J. Appl. Polym. Sci.* **1959**, *1*, 164–168.
- (3) Linton, W. H.; Goodman, H. H. *J. Appl. Polym. Sci.* **1959**, *1*, 179–184.
- (4) Masamoto, J. *Prog. Polym. Sci.* **1993**, *18*, 1–84.
- (5) Alamo, R. G.; VanderHart, D. L.; Nyden, M. R.; Mandelkern, L. *Macromolecules* **2000**, *33*, 6094–6105.
- (6) Takahashi, M.; Tashiro, K.; Amiya, S. *Macromolecules* **1999**, *32*, 5860–5871.
- (7) VanderHart, D. L.; Pérez, E. *Macromolecules* **1986**, *19*, 1902–1909.

- (8) VanderHart, D. L.; Simmons, S.; Gilman, J. W. *Polymer* **1995**, *36*, 4223–4232.
- (9) VanderHart, D. L.; Orts, W. J.; Marchessault, R. H. *Macromolecules* **1995**, *28*, 6394–6400.
- (10) Pérez, E.; VanderHart, D. L. *J. Polym. Sci., Part B: Polym. Phys.* **1987**, *25*, 1637–1653.
- (11) Yoshie, N.; Sakurai, M.; Inoue, Y.; Chûjô, R. *Macromolecules* **1992**, *25*, 2046–2048.
- (12) Iguchi, M. *Makromol. Chem.* **1976**, *177*, 549–566.
- (13) Everaert, V.; Groeninckx, G.; Koch, M. H. J.; Reynaers, H. *Polymer* **2003**, *44*, 3491–3508.
- (14) Tadokoro, H.; Yasumoto, T.; Murahashi, S.; Nitta, I. *J. Polym. Sci.* **1960**, *44*, 266–269.
- (15) Uchida, T.; Tadokoro, H. *J. Polym. Sci., Part A2* **1967**, *5*, 63–81.
- (16) Takahashi, Y.; Tadokoro, H. *J. Polym. Sci., Polym. Phys. Ed.* **1979**, *17*, 123–130.
- (17) Tashiro, K.; Kamae, T.; Asanaga, H.; Oikawa, T. *Macromolecules* **2004**, *37*, 826–830.
- (18) Alexander, L. E. *X-ray Diffraction Methods in Polymer Science*; Wiley-Interscience: New York, 1969.
- (19) Demco, D. E.; Johansson, A.; Tegenfeldt, J. *Solid State Nucl. Magn. Reson.* **1995**, *4*, 13–38.
- (20) Packer, K. J.; Poplett, I. J. F.; Taylor, M. J. *J. Chem. Soc., Faraday Trans. 1* **1988**, *84*, 3851–3863.
- (21) Kenwright, A. M.; Packer, K. J.; Say, B. J. *J. Magn. Reson.* **1986**, *69*, 426–439.
- (22) Mellinger, F.; Wilhelm, M.; Spiess, H. W. *Macromolecules* **1999**, *32*, 4686–4691.
- (23) Veeman, W. S.; Menger, E. M. *Bull. Magn. Reson.* **1980**, *2*, 77.
- (24) Cholli, A. L.; Ritchey, W. M.; Koenig, J. L. *Spectrosc. Lett.* **1983**, *16*, 21–28.
- (25) Hirai, A.; Horii, F.; Kitamaru, R.; Fatou, J. G.; Bello, A. *Macromolecules* **1990**, *23*, 2913–2917.
- (26) Schmidt, A.; Veeman, W. S.; Litvinov, V. M.; Gabriëlse, W. *Macromolecules* **1998**, *31*, 1652–1660.
- (27) Cesari, M.; Perego, G.; Mazzei, A. *Makromol. Chem.* **1965**, *83*, 196–206.
- (28) Imada, K.; Miyakawa, T.; Chatani, Y.; Tadokoro, H.; Murahashi, S. *Makromol. Chem.* **1965**, *83*, 113–128.
- (29) Cui, M.-H.; Zhang, Y.; Werner, M.; Yang, N.-L.; Fenelli, S. P.; Grates, J. A. *Polym. Prepr.* **2001**, *42*, 21–22.

MA062507L